

# Long-period fiber grating effects induced by double-sided loading

Tsung-Yi Tang

Pao-Yi Tseng

Chung-Yi Chiu

Chih-Nan Lin

C. C. Yang, MEMBER SPIE

Yean-Woei Kiang

National Taiwan University

Department of Electrical Engineering

Graduate Institute of Electro-Optical

Engineering

and

Graduate Institute of Communication

Engineering

1, Roosevelt Road, Section 4

Taipei, Taiwan

E-mail: ccy@cc.ee.ntu.edu.tw

Kung-Jen Ma

Chung Hua University

Department of Mechanical Engineering

Hsinchu, Taiwan

**Abstract.** Periodical perturbations along an optical fiber can cause power coupling between the core and cladding modes for the applications of spectral filtering and derivative operations. Such perturbations can be generated through periodical loading on fiber. By applying loading onto a fiber with two face-to-face, identical groove structures, it was found that the long-period grating effects were dependent on the relative phase of the two periodical corrugations. Particularly, when the relative phase was zero (crest to crest), spectral filtering effects disappeared completely. The comparisons of such results between the cases of jacketed and unjacketed fibers led to the conclusion that geometric deformation, instead of direct pressure-induced effects, was the dominating mechanism for generating spectral filtering functions in the double-sided loading configuration. The same conclusion can be applied to a single-sided loading device. © 2003 Society of Photo-Optical Instrumentation Engineers. [DOI: 10.1117/1.1578647]

Subject terms: long-period fiber grating; mode coupling; microbending.

Paper 020239 received Jun. 11, 2002; revised manuscript received Jan. 2, 2003; accepted for publication Jan. 3, 2003.

## 1 Introduction

Spectral filtering and its derivative operations, such as gain flattening, are important functions for fiber communication applications.<sup>1-5</sup> Spectral filtering can be implemented with long-period fiber gratings of various forms. In a long-period fiber grating with phase matching, the core-mode signal in the fiber can be coupled into cladding modes, resulting in spectral depressions.<sup>6</sup> Effective long-period fiber gratings can be realized with permanent modifications of the fiber, such as etching<sup>7</sup> and UV-induced refractive index changes,<sup>8</sup> and temporary alteration of fiber propagation characteristics. The method of temporary alteration has the advantage of dynamically controlling the function of spectral filtering. Dynamic long-period fiber gratings can be implemented through the application of either an acoustic wave to the fiber,<sup>9-12</sup> or periodical loading onto the fiber.<sup>13-15</sup> In the loading technique, two possible mechanisms may result in the aforementioned phase matching process, including geometric deformation (microbending) and pressure effects for periodical refractive index variation of the fiber.

We report the spectral filtering results of effective long-period gratings implemented by double-sided loading with two identical blocks of periodical grooves. Also, the dominating mechanism for effective grating effects is discussed. In our experiments, it was found that the positions and depths of transmission spectral depressions varied with the relative phase of the two periodically grooved structures. When the two periodical structures are exactly in phase, i.e., crests are exactly matched, all spectral depressions disappear. This is true whether the plastic jacket is removed or not. This observation leads to the conclusion that geometric deformation is the dominating mechanism for phase match-

ing between the core and cladding modes. The conclusion is further confirmed with the results of single-sided loading on fibers, which manifests that loading without a plastic jacket is less effective than the case with a jacket. The jacket is supposed to provide the means for microbending, which results in effective mode coupling. In addition, a theoretical study on the coupling behaviors induced by microbending shows reasonably consistent results with the experimental data.

The work is organized as follows. In Sec. 2, the experimental procedures and major results are presented. Then, interpretations for the results are discussed in Sec. 3. Finally, conclusions are drawn in Sec. 4.

## 2 Experimental Procedures and Results

As shown in Fig. 1, for double-sided loading, two identical copper blocks of  $3 \times 3 \times 0.5$  cm ( $L \times W \times T$ ) with periodical corrugations on the  $L \times W$  plane were prepared. Square grooves of  $400 \mu\text{m}$  in depth, 50% in duty cycle, and  $700 \mu\text{m}$  in period were fabricated with mechanical processes. A commonly used communication fiber (Corning, SMF-28) was placed between the two corrugated copper blocks. Loading was applied by moving one of the blocks toward the other with a translation stage. The relative position, i.e.,  $x$  shown in Fig. 1, corresponding to the relative phase of the two face-to-face corrugated blocks, was controlled by a translation stage moving along another direction. The fiber was aligned along the normal to the groove lines. The transmission spectrum of the fiber under loading was recorded with an HP spectrum analyzer (HP 70004A) with a spectral resolution of  $0.08 \text{ nm}$ .

Figure 2 shows the normalized transmission spectra of two loading levels: 0.15 and 0.2 mm stage displacements

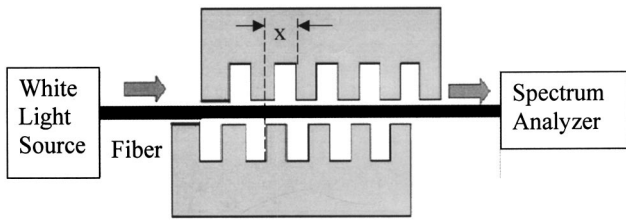


**Fig. 1** Experimental setup for double-sided loading on a fiber. The distance  $x$  corresponds to the relative phase of the two grooves.

for the upper and lower curves, respectively. In this situation, the relative phase of the two blocks was about  $\pi/2$ . Note that zero phase is defined as the situation when crests of the two corrugated blocks are exactly matched. The spectra shown in Fig. 2 were normalized to the level of zero loading (completely loose). Three depressions around 1500, 1560, and 1620 nm can be clearly seen. A deeper depression corresponds to stronger coupling between the core and cladding modes.

The wavelengths and depths of the spectral depression minima were recorded when the relative phase of the two corrugated blocks was varied. Figures 3 and 4 show the variations of depression wavelength and depth with the relative phase when the loading level is about 0.22 mm in stage displacement. Here, the relative phase is also displayed with the stage displacement in millimeters. In either Figs. 3 or 4, periodical variations with a period of 700  $\mu\text{m}$  can be clearly seen, confirming the 700- $\mu\text{m}$  corrugation period. Only two coupling wavelengths are shown because the one near 1500 nm is unclear (see Fig. 2). The other abscissa in either Figs. 3 or 4 indicates the corresponding relative phase. One can clearly see that near the phases of integer numbers of  $2\pi$ , all the induced spectral depressions disappear. It is noted that the depression wavelength reaches the largest value when the relative phase is an odd number of  $\pi$ . In this situation, coupling is expected to be strongest because the depression depth increases as the

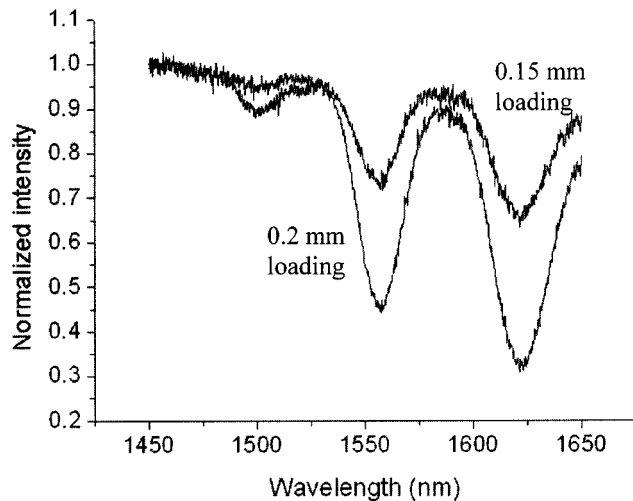


**Fig. 2** A typical normalized transmission spectrum of double-side loaded fiber grating with a corrugation period of 700  $\mu\text{m}$ . The loading displacements for the two curves are 0.15 and 0.2 mm. The relative phase of the two periodical corrugations is about  $\pi/2$ .

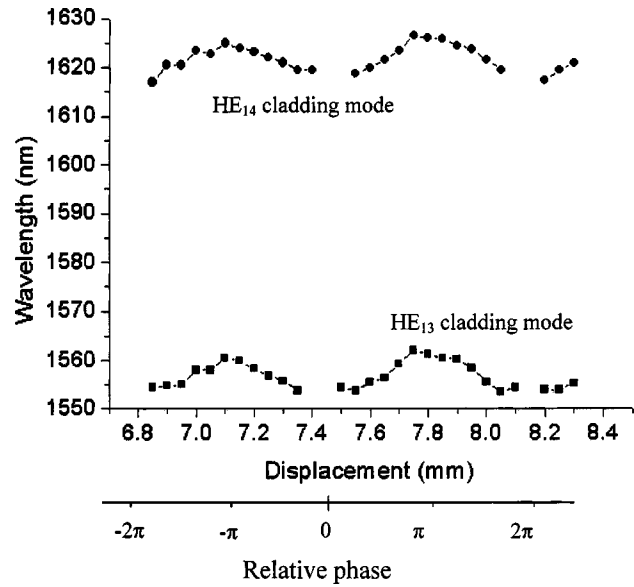


**Fig. 3** Variations of the wavelengths of spectral depression minima with the relative phase of the two periodical corrugations when the loading level is 0.22 mm. Two abscissas represent the physical displacement and the relative phase of the two periodical corrugations.

relative phase moves away from integer numbers of  $2\pi$ , as shown in Fig. 4. The tuning range in varying the relative phase is about 10 nm. Such wavelength variations can be attributed to the change of effective fiber propagation constant in loading with different relative corrugation phases. As shown in Fig. 4, the spectral depression depth drops fast when the relative phase approaches an integer number of  $2\pi$ . The minimum features of depression depth near odd numbers of  $\pi$  relative phase may originate from the saturation effects of loading. Note that the nonsmooth data point variations in Figs. 3 and 4 can be attributed to the imperfect periodical groove structures.

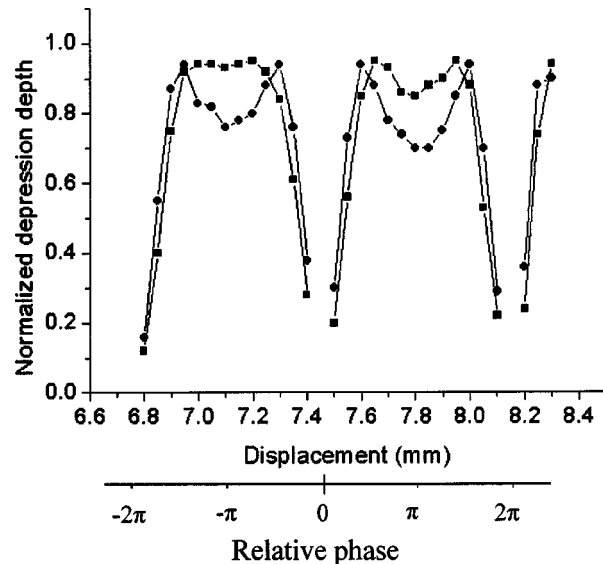


**Fig. 4** Variations of the depths of spectral depression minima with the relative phase of the two periodical corrugations. The two datasets correspond to those of Fig. 3.

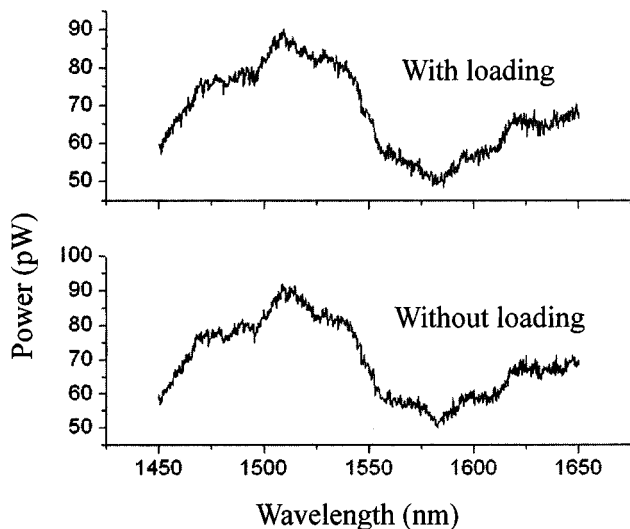


**Fig. 5** Transmission spectra of the case with zero relative phase for unloaded (the lower curve) and 0.22 mm displacement loading (the upper curve) conditions. The fiber jacket is not removed.

Figure 5 shows the comparison of spectra between the cases without loading (the lower curve) and with loading (the upper curve, with 0.22 mm stage displacement loading level—a relatively high loading level) when the relative phase is an integer number of  $2\pi$ . We can see the almost identical spectra (even without a significant difference in background level), which do not have any significant spectral depression. The ratio of the two curves results in  $<7\%$  noise fluctuation within the spectral range from 1.4 through 1.7  $\mu\text{m}$ . Such results confirm the insignificant effect of loading when the relative phase is an integer number of  $2\pi$ .

### 3 Discussions

The insignificant loading effect in the case where the relative phase is an integer number of  $2\pi$  has an important implication. The application of loading onto fibers may produce two mechanisms for inducing mode coupling: geometric deformation and a pressure-induced elasto-optical effect. The former forms microbending and the latter produces periodical refractive index variation. From the results described previously, we may conclude that geometric deformation is the dominating mechanism for mode coupling in our loading configuration. This conclusion can be understood in Figs. 6(a) and 6(b). In Fig. 6(a), the loading effect on fiber with a zero relative phase is schematically depicted. Here, one can see that the loading effect is essentially the periodical application of pressure onto fiber. Such a pressure may not be effectively applied to the glass portion of the fiber, because the plastic jacket may absorb the pressure. On the other hand, as shown in Fig. 6(b), the loading effect on fiber with a  $\pi$  phase is essentially geometric deformation, i.e., microbending. Such a geometric deformation produces significant coupling between the core and cladding modes, as shown in Figs. 3 and 4. When the relative phase moves from  $\pi$  to zero, the microbending amplitude is reduced and the effective grating period is decreased. Therefore, the coupling strength, i.e., spectral depression depth, is reduced, as shown in Fig. 4. Also, the

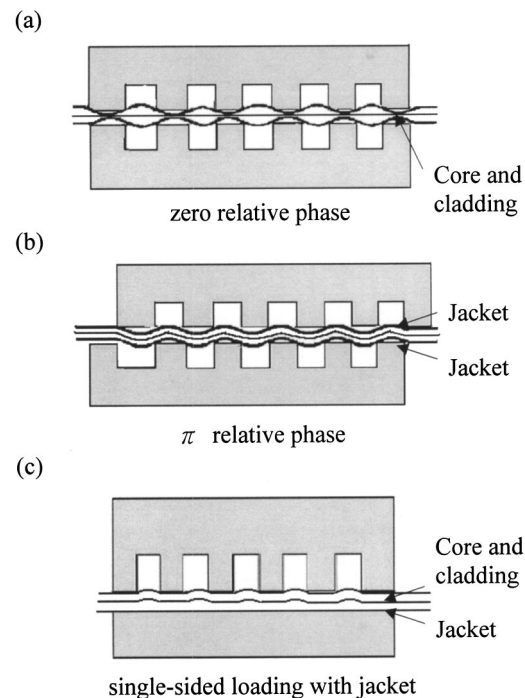


**Fig. 6** Schematic drawings of fiber deformations in the cases of (a) zero and (b)  $\pi$  relative phases of the two periodical corrugations in double-sided loading and (c) in the case of single-sided loading. Microbending is expected in the cases of (b) and (c).

depression wavelength becomes shorter when the relative phase moves from  $\pi$  to zero, as shown in Fig. 3.

As mentioned, one may wonder that the insignificant loading effect in the case of zero relative phase may originate from the pressure absorption of the fiber jacket. To understand the jacket effects, we removed the jacket and conducted the loading experiments. We observed almost the same results, except that the loading level could not be too large, otherwise the fiber was broken. Particularly, an insignificant loading effect could again be observed in the case of zero relative phase. The transmission spectra of the unloaded and loaded (loading level 1.2 mm) cases look almost identical, as shown in Fig. 7.

The observations described so far may bring doubts about the effects of single-sided loading.<sup>15</sup> By intuition, single-sided loading cannot create microbending of fibers and its grating effects must come from periodical pressure distribution. To clarify this point, we also conducted single-sided loading with jacketed and unjacketed fibers. Figure 8 shows the loading results with the solid curve for the case with a jacket and the dashed curve for the case without a jacket. We did observe the grating effects with single-sided loading, either with or without a jacket. However, the loading effect with a jacket was much more significant. The results in Fig. 8 ruled out the possible effect of periodical pressure in loading because the existence of a jacket, which was supposed to absorb pressure, resulted in much stronger grating effects. Such a result can only be explained by the conclusion that even in the case of single-sided loading, the dominating mechanism for mode coupling is microbending. As depicted in Fig. 6(c), the elasticity of the jacket can help the fiber to become curved when the corrugated structure is

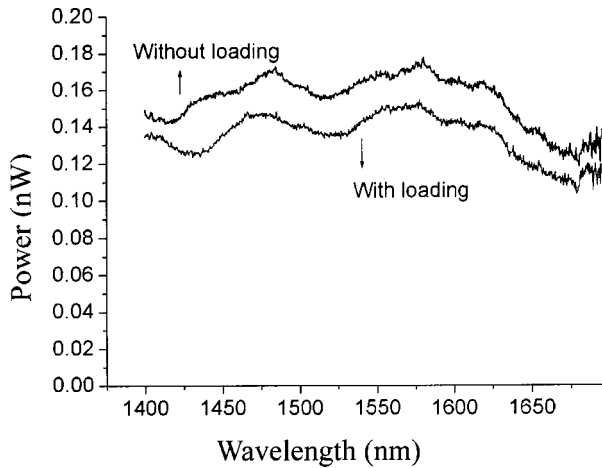


**Fig. 7** Transmission spectra of the case with zero relative phase for unloaded (the upper curve) and 0.12 mm displacement loading (the lower curve) conditions. The fiber jacket is removed.

applied. When the jacket is removed, it becomes difficult to produce microbending on rigid glass.

To further make sure that the spectral depressions in Fig. 2 were really due to the coupling of the core mode and various cladding modes under microbending, we conducted a theoretical study on the coupling behaviors in a fiber with microbending. The coupling behaviors between the core and cladding modes due to microbending are quite different from those in a long-period fiber grating with a periodical effective refractive index variation in the core.<sup>6</sup> With a perturbation method, it can be shown that a  $HE_{v\mu}$  cladding mode with  $v=2$  leads to a longitudinal coupling coefficient variation of the same period as microbending. However, a  $HE_{v\mu}$  cladding mode with  $v=1$  results in a coupling coefficient variation of one half the period of microbending. Such results are due to the odd and even nature of the cladding modes with  $v=2$  and 1, respectively. The detailed discussions of the coupling behaviors will be presented in another publication. Here, we simply demonstrate a result simulating the experimental data. We assumed a 3-cm, long-period fiber grating of microbending with a period of

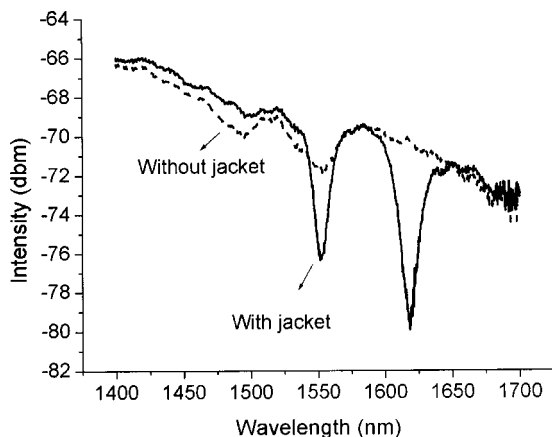


**Fig. 8** Transmission spectra of a single-side loaded fiber in the cases of keeping the jacket (solid curve) and removing the jacket (dashed curve).

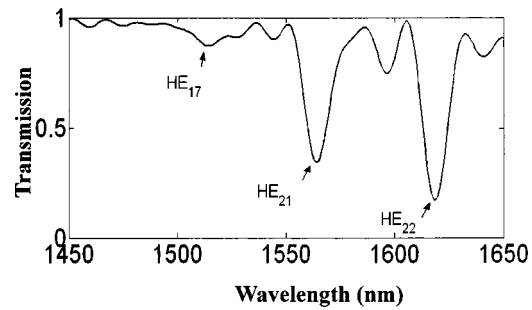


**Fig. 9** Numerical results of the transmission spectrum showing the coupling between the core and cladding modes.

700  $\mu\text{m}$  and 10% bending (the fiber axis deviates from the unperturbed situation by 10% of the core radius). The radii of the fiber core and cladding were assumed to be 4.1 and 62.5  $\mu\text{m}$ , respectively. The refractive indices of the core, cladding, and jacket were 1.44919, 1.44408, and 1, respectively. It was found that the coupling results with the low-order cladding modes were weakly dependent on the refractive index of the jacket. With little effect on the results, we set the jacket refractive index as 1 (free space). The results of a normalized transmission spectrum from numerical calculations are shown in Fig. 9. Here, three major depressions can be clearly seen, with the depression minima at around 1510, 1560, and 1620 nm. These three major depression wavelengths are quite consistent with those of the three depressions in Fig. 2. Also, the relative depths basically agree between the experimental and numerical results. From this comparison, we can identify that the three depressions observed in the experiment originate from the coupling of the core mode ( $HE_{11}$ ) with the cladding modes  $HE_{17}$ ,  $HE_{21}$ , and  $HE_{22}$  (see Fig. 9), respectively. Note that the coupling of the  $HE_{17}$  mode is phase matched with the coupling coefficient period of 350  $\mu\text{m}$ . Those of the  $HE_{21}$  and  $HE_{22}$  modes were phase matched with the coupling coefficient period of 700  $\mu\text{m}$ .

#### 4 Conclusions

In summary, we demonstrate the spectral filtering effects of fiber with double-sided loading of periodical corrugations. It was found that the filtering wavelength and strength were dependent on the relative phase of the two periodical corrugations. In particular, when the relative phase was zero (crest to crest), spectral filtering effects disappeared completely. Such results and other evidences led to the conclusion that geometric deformation, instead of direct pressure-induced effects, was the dominating mechanism for generating spectral filtering functions in the double-sided loading configuration. Such a conclusion should also be true for the configuration of single-sided loading.

#### Acknowledgments

This research was supported by the National Science Council, The Republic of China, under the grants of NSC 89-2218-E-002-094, NSC 89-2218-E-002-095, and NSC 89-2215-E-002-051.

## References

1. M. Tachibana, R. I. Laming, P. R. Morkel, and D. N. Payne, "Erbium-doped fiber amplifier with flattened gain spectrum," *IEEE Photonics Technol. Lett.* **3**(2), 118–120 (1991).
2. M. K. Pandit, K. S. Chiang, Z. H. Chen, and S. P. Li, "Tunable long-period fiber gratings for EDFA gain and ASE equalization," *Microwave Opt. Technol. Lett.* **25**(3), 181–184 (2000).
3. C. Y. Lin and L. A. Wang, "A wavelength- and loss-tunable band-rejection filter based on corrugated long-period fiber grating," *IEEE Photonics Technol. Lett.* **13**(4), 332–334 (2001).
4. J. H. Song, Y. Taguchi, M. Sasaki, and K. Hane, "Tunable wavelength filter using fiber Bragg gratings combined with a surface micromachining technology," *Proc. SPIE* **4416**, 478–481 (2001).
5. I. B. Sohn, N. K. Lee, H. W. Kwon, and J. W. Song, "Tunable gain-flattening filter using microbending long-period fiber gratings," *Opt. Eng.* **41**(7), 1465–1466 (2002).
6. T. Erdogan, "Cladding-mode resonances in short- and long-period fiber grating filters," *J. Opt. Soc. Am. A* **14**(7), 1760–1773 (1997).
7. S. A. Vasiliev, E. M. Dianov, D. Varelas, H. G. Limberger, and R. P. Salathe, "Postfabrication resonance peak positioning of long-period cladding-mode-coupled gratings," *Opt. Lett.* **21**(22), 1830–1832 (1996).
8. A. M. Vengsarkar, P. J. Lemaire, J. B. Judkins, V. Bhatia, T. Erdogan, and J. E. Sipe, "Long-period fiber gratings as band-rejection filter," *J. Lightwave Technol.* **14**(1), 58–65 (1996).
9. R. Faced, C. Alegria, M. N. Zervas, and R. I. Laming, "Acoustooptic attenuation filters based on tapered optical fibers," *IEEE J. Sel. Top. Quantum Electron.* **5**(5), 1278–1288 (1999).
10. D. W. Huang, W. F. Liu, C. W. Wu, and C. C. Yang, "Reflectivity-tunable fiber Bragg grating reflectors," **12**(2), 176–178 (2000).
11. W. F. Liu, I. M. Liu, L. W. Chung, D. W. Huang, and C. C. Yang, "Acoustics-induced reflection wavelength switching in a fiber Bragg grating," *Opt. Lett.* **25**(18), 1319–1321 (2000).
12. A. Diez, T. A. Birks, W. H. Reeves, B. J. Mangan, and P. St. J. Russell, "Excitation of cladding modes in photonic crystal fibers by flexural acoustic waves," *Opt. Lett.* **25**(20), 1499–1501 (2000).
13. R. C. Youngquist, J. L. Brooks, and H. J. Shaw, "Birefringent-fiber polarization coupler," *Opt. Lett.* **8**(6), 656–658 (1983).
14. R. C. Youngquist, J. L. Brooks, and H. J. Shaw, "Two-mode fiber modal coupler," *Opt. Lett.* **9**(2), 177–179 (1984).
15. S. Savin, M. J. F. Digonnet, G. S. Kino, and H. J. Shaw, "Tunable mechanically induced long-period fiber gratings," *Opt. Lett.* **25**(10), 710–712 (2000).

**Tsung-Yi Tang** received his BS degree in electrical engineering from National Taiwan University, Taipei, in June 2002. Currently, he is working on his MS degree in the Graduate Institute of Electro-Optical Engineering, National Taiwan University. His research interests include fiber grating, optical coherence tomography and nitride material characterization.

**Pao-Yi Tseng** received her BS degree in electrical engineering from National Taiwan University, Taipei, in June 2001. Currently, she is working in the Department of Electrical Engineering, National Tai-

wan University as a full-time teaching assistant. Her research interests include fiber grating and optical coherence tomography.

**Chung-Yi Chiu** received his BS degree in communication engineering from National Chiao Tung University, Hsinchu, Taiwan, in June 2001. Currently, he is working on his MS degree in the Graduate Institute of Electro-Optical Engineering, National Taiwan University, Taipei. His research interests include numerical modeling of fiber grating and related components.

**Chih-Nan Lin** received his BS degree in electrical engineering from National Central University, Chung-Li, Taiwan, in June 2000, and his MS degree in communication engineering from National Taiwan University, Taipei, in July 2002. His research interests include numerical modeling of fiber grating and related components.

**C. C. Yang** received his BS degree in electrical engineering from National Taiwan University, Taipei, in 1976, and then BS and PhD degrees also in electrical engineering from University of Illinois, Urbana-Champaign, in 1981 and 1984, respectively. He became an assistant professor of electrical engineering at The Pennsylvania State University, University Park, in 1984. There, he received his tenure and promotion to the rank of associate professor in 1990. In 1993, he joined National Taiwan University as a professor of electro-optical engineering and electrical engineering. Since August 2001, he has been the Director of the Institute of Electro-Optical Engineering, National Taiwan University. His research interests include fiber grating related components, nanotechnologies, nitride compounds, photonic crystals, and biomedical photonics. He has published more than 400 journal and conference papers. He is a member of SPIE, a senior member of IEEE LEOS, and a fellow of OSA.

**Yean-Woei Kiang** received the BSEE, MSEE, and PhD degrees from National Taiwan University, Taipei, in 1977, 1979, and 1984, respectively. In 1979, he joined the faculty of the Department of Electrical Engineering, National Taiwan University, where he is currently a professor. His research interests include wave propagation, scattering, inverse scattering, and optoelectronics.

**Kung-Jen Ma** received his PhD degree at the University of Birmingham, United Kingdom in July 1997. He worked at Chung-Cheng Institute of Technology and set up the High-Resolution Transmission Electron Microscopy Laboratory and an excimer laser micromachining system from 1997 to 2002. Now he is an associate professor of mechanical engineering at Chung Hua University. His research fields include nanomaterials, plasma surface engineering, the phase transformation of materials, and micromachining.